Environmental Science & Technology

Article

pubs.acs.org/est

GHGfrack: An Open-Source Model for Estimating Greenhouse Gas Emissions from Combustion of Fuel during Drilling and Hydraulic Fracturing

Kourosh Vafi* and Adam Brandt

Department of Energy Resources Engineering, Stanford University, Stanford, California 94305, United States

Supporting Information

ABSTRACT: This paper introduces *GHGfrack*, an open-source engineering-based model that estimates energy consumption and associated GHG emissions from drilling and hydraulic fracturing operations. We describe verification and calibration of *GHGfrack* against field data for energy and fuel consumption. We run *GHGfrack* using data from 6927 wells in Eagle Ford and 4431 wells in Bakken oil fields. The average estimated energy consumption in Eagle Ford wells using lateral hole diameters of 8 $^{3}/_{4}$ and 6 $^{1}/_{8}$ in. are 2.25 and 2.73 TJ/well, respectively. The average estimated energy consumption in Bakken wells using hole diameters of 6 in. for horizontal section is 2.16 TJ/well. We estimate average greenhouse gas (GHG) emissions of 419 and 510 tonne of equivalent CO_2 per well (tonne of CO_2 eq/well) for the two aforementioned assumed geometries in Eagle Ford, respectively, and 417 tonne of CO_2 eq/well for the case of Bakken. These estimates are limited only to GHG emissions from combustion of diesel fuel to supply energy only for rotation of drill string, drilling mud circulation, and fracturing pumps. Sensitivity analysis of the model shows that the top three key variables in driving energy intensity in drilling are the lateral hole diameter, drill pipe internal diameter, and mud flow rate. In hydraulic fracturing, the top three are lateral casing diameter, fracturing fluid volume, and length of the lateral.

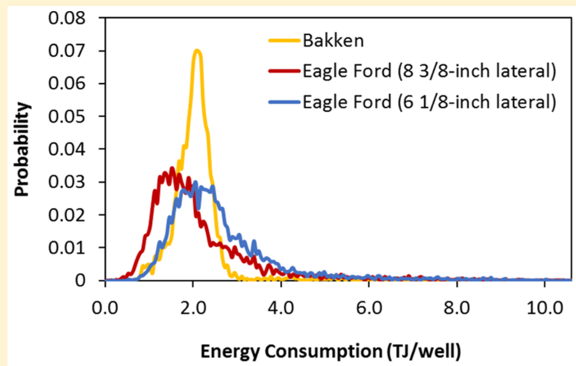

1. INTRODUCTION

Hydraulic fracturing increases the effective recovery of oil and gas from formations with low permeability. Combined with horizontal drilling, hydraulic fracturing has resulted in profound increases in U.S. oil and natural gas production in recent years, resulting in a reversal of a nearly 40-year decline in U.S. oil output. According to the U.S. Energy Information Administration (EIA), 64% of total U.S. natural gas production in 2013 is tight gas, shale gas, and gas from tight oil.[1] In the same year, 42% of total U.S. oil production has been tight oil.[1] EIA foresees the production of natural gas from shale and tight formations to increase above 70% and tight oil above 50% by 2020.[1]

Despite this success, there has been significant controversy over environmental impacts of hydraulic fracturing. These impacts include GHG emissions, criteria air pollutant emissions, impacts on water resources, fresh water consumption, and land use or habitat impacts. Fracturing requires significant energy inputs, resulting in emissions of GHGs and particulate matter from diesel engines. Other concerns exist with regard to water contamination from hydraulic fracturing.[2]

Before fracturing, the well must be drilled and protective casing must be cemented into the vertical and (sometimes) horizontal portions of the well. A typical well consists of multiple vertical sections with different hole diameters, a curved section in which the drilling angle goes from near-vertical to near-horizontal, and a horizontal section of often significant length.

After the well is drilled and completed, fracturing pumps are used to inject high-pressure water into the horizontal section of the well, creating fissures in the productive formation. The water is mixed with fracturing sand, or proppant, and other chemicals that serve as lubricants, viscosity-adjusting agents, scale reducers, and biocides.

Because of the importance of hydraulic fracturing in current and future North American hydrocarbon production, there is a strong need to understand the impacts of fracturing operations on air for regulatory purposes. For example, the California Low Carbon Fuel Standard (LCFS) assesses different crude oils using an open-source GHG estimation tool but does not currently assess the impacts of hydraulic fracturing.[3,4] Current methods for assessing GHG emissions from oil and gas operations do not carefully model drilling and fracturing operations.[3,4] Thus, we have created *GHGfrack*, an open-source model for computing GHG emissions from drilling and hydraulic fracturing operations. *GHGfrack* represents a large advance over current life cycle accounting methods for oil and

Received: April 19, 2016
Revised: June 21, 2016
Accepted: June 24, 2016
Published: June 24, 2016

DOI: 10.1021/acs.est.6b01940
Environ. Sci. Technol. 2016, 50, 7913−7920

gas drilling operations, because it applies detailed engineering methods in place of previously used simple models that cannot account for variability in drilling practice or well characteristics.

In this paper, we describe modules in *GHGfrack* that estimate the energy consumption required for three key energy uses: rotating the drill string, maintaining drilling fluid circulation, and pumping of fracturing fluid. The estimated GHG emissions are limited to emissions from combustion of diesel fuel to supply these energies. We therefore do not include fugitive methane emissions in the current estimate. The GHG emissions from other sources like flow back processes[5] or underbalanced drilling[6] can be significant. These emission sources require an independent research effort and could be added to a future extension of *GHGfrack*. Also, the model does not address the emissions from transportation, site preparation, and land use change as they are studied and covered by other LCA models.[3,4]

After explaining the mathematical foundation of *GHGfrack*, we discuss verification and calibration of the model. We then demonstrate the power of *GHGfrack* in handling a large number of wells by running it on data from several thousand wells in the Bakken and Eagle Ford formations of North Dakota and Texas. We compare and discuss the resulting GHG emissions from energy consumption distributions for these two oil fields. We conclude with a sensitivity analysis to identify the key model input variables.

2. METHODS

GHGfrack can be used to model energy requirements for drilling and fracturing of wells in both gas and oil fields. Each field will have different model input variables that describe the operating conditions and the formation characteristics. The operating conditions and well geometry can change during the drilling and hydraulic fracturing operation. In *GHGfrack*, the user can define as many as drilling sections as necessary to follow this change and assign different model inputs (i.e., well diameter, mud flow rate, pipe roughness, etc.) to each section. For example, if an operator changes the set mud flow rate five times during drilling, the well can be divided into five sections with different mud flow rates. In modeling hydraulic fracturing, *GHGfrack* lets the user define the geometry of the well, the number of fracturing stages, and the operating conditions freely. See the Supporting Information for a glossary of the technical terms.

2.1. Rotation of the Drill String. The energy for rotation of the drill bit can be supplied by rotating either the drill string, a downhole mud motor, or both. The *GHGfrack* drilling module computes the energy requirement for rotating the drill string. Mechanical energy from an engine is transferred to the drill string through a rotary table or top-drive system on the drill-rig deck. The brake horsepower (BHP) of the top driver is calculated by eq 1:[7]

$$\mathrm{BHP} = \frac{2\pi TN}{33000\eta} \tag{1}$$

where T is the torque (ft $\mathrm{lb_f}$), N is the rotational speed of the drill string (rpm), and η (dimensionless) is the overall efficiency of the power transmission from the engine to the drill string through all electromechanical components. The rotational torque requirement in vertical wells is generally less than 15000 ft $\mathrm{lb_f}$ but in directional wells can exceed 80000 ft $\mathrm{lb_f}$.[7] The rate of penetration (ROP) is the speed of progress of the drill bit through rock (ft/min). Given the depth of each drilling section and ROP, the drilling time for that section can be calculated and used to calculate the energy consumption based on the estimated BHP for that section.

2.2. Drilling Fluid Hydraulics Module. Drilling fluid performs many functions: cooling and lubricating of the drill bit, removing drill cuttings, ensuring the stability of the wellbore given significant pressures in the deep subsurface, sealing permeable formation during drilling to prevent fluid influx or blowouts, and providing energy to downhole motors to drive drill bit rotation. Drilling fluid can be a gas, a liquid, or a two-phase fluid (mist, foam, and gasified mud).[7] The current version of *GHGfrack* considers only drilling muds. Figure 1 shows the flow of mud through the drill pipe, drill collar, drill bit, and annulus. The energy balance equation between points A and B in Figure 1 can be written as[7]

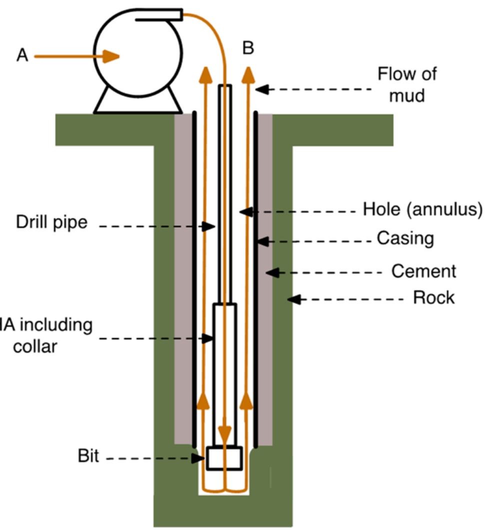

Figure 1. Mud circulation.

$$\frac{\rho g h_A}{g_c} + \frac{\rho {V_A}^2}{2g_c} + P_A + \mathcal{W}_p - \mathcal{W}_f - \mathcal{W}_{dm} = \frac{\rho g h_B}{g_c} + \frac{\rho {V_B}^2}{2g_c} + P_B \tag{2}$$

where $\mathcal{W}$ is work spent or lost per unit volume of fluid and has dimensions equal to pressure ($\mathrm{lb_f/ft^2}$), P is the pressure ($\mathrm{lb_f/ft^2}$), ρ is the density of mud ($\mathrm{lb_m/ft^3}$), V is the velocity of fluid (ft/s), h is the elevation (ft), and g_c is the coefficient for conversion of $\mathrm{lb_m}$ to $\mathrm{lb_f}$. This equation can be simplified to eq 3 to calculate the pump differential pressure:

$$\Delta P_{pump} = \Delta P_{friction} + \Delta P_{dynamic} + \Delta P_{dm} - \Delta P_{hydrostatic} + \Delta P_{other} \tag{3}$$

In this equation, subscripts dm and friction represent downhole motor and pipe friction, respectively.

As Figure 1 shows, the hydrostatic pressure difference, $\Delta P_{hydrostatic}$, is zero because of the equal height of the mud level in the drill string and the annulus. Any difference between the level of the mud pump suction A and the annulus output B plus pressure drop through the fittings can be considered as ΔP_{other}. The pressure drop of the downhole motor, ΔP_{dm}, can be

DOI: 10.1021/acs.est.6b01940
Environ. Sci. Technol. 2016, 50, 7913−7920

estimated using the performance diagrams that the manufacturer provides for each model and is related to the mud flow rate, rotary speed, and rotational torque.[8] Equations 2 and 3 show that the conversion of the energy of flowing mud to the rotational energy of the drill bit requires increasing the pump discharge pressure by ΔP_{dm} psi and thus increasing pump BHP.

A significant source of dynamic pressure drop is the flow of the mud through the drill bit nozzles.[7] *GHGfrack* computes the pressure drop of the fluid through the nozzles by[7]

$$\Delta P_{\text{drill bit}} = \frac{8.3 \times 10^{-5} \gamma Q^2}{C_d^{\,2} A_t^{\,2}} \tag{4}$$

where Q is the flow rate (gpm), γ is the mud density (lb_f/gal), C_d is the dimensionless nozzle discharge coefficient, and A_t is the area of the jets open to the flow (in.^{2}).

Drilling fluids are non-Newtonian in shear behavior and are usually modeled as Bingham plastics or power law fluids.[7] *GHGfrack* models the rheology of these two types of non-Newtonian fluids for laminar and turbulent regimes for both pipe and annular flow. These models are used to calculate the pressure drop of mud flow due to pipe friction, which is a significant source of drilling energy consumption. For the case studies in this paper, we assume that the drilling mud follows the popular Bingham plastics model. As an example, eq 5 calculates the pressure drop due to friction in a pipe in a laminar flow regime:[7]

$$\Delta P_{fp} = \frac{\mu_p V}{1500 D_{ip}^{\,2}} + \frac{\tau_y}{255 D_{ip}} \tag{5}$$

where ΔP_{fp} is the pressure drop in the pipe (psi/ft), μ_p is the plastic viscosity (cP), τ_y is the yield stress (lb_f/100 ft^2)], V is the average velocity in the pipe (ft/s), and D_{ip} is the internal diameter of the pipe (in.).

The mathematical derivation of the equation for friction pressure loss in laminar annular flow for non-Newtonian fluids with a yield value is quite complex. Therefore, Azar and Samuel[7] suggest approximating the annular flow by slot flow (flow between two flat plates). It can be shown that the annular flow can be accurately approximated by a slot flow when the ratio of the diameter of the pipe to hole diameter is >0.3. This condition is generally met in drilling applications.[7] The equation for annular friction loss thus becomes (laminar regime)

$$\Delta P_{fa} = \frac{\mu_p V}{1000 (D_{hole} - D_{op})^2} + \frac{\tau_y}{255 (D_{hole} - D_{op})} \tag{6}$$

where ΔP_{fa} is the pressure drop in the annulus (psi/ft), D_{op} is the internal diameter of the pipe (in.), and D_{hole} is the diameter of the hole (in.). Other parameters are defined as in eq 5.

We use eq 7 to calculate the Fanning friction factor for the turbulent flow of a Bingham plastic in a pipe or annulus:[9]

$$f = A(\text{Re})^{-B} \tag{7}$$

in which Re is the Reynolds number. See the Supporting Information for the procedure that determines the value of parameters A and B (section 1 of the Supporting Information, eqs S1−S7).

Knowing the flow rate of mud Q is essential in the calculation of the frictional pressure drop in the pipe, nozzle, and downhole motor. When the mud flow rate and pressure drop are known, the mud pump BHP can be calculated:[7]

$$\text{BHP} = \frac{\Delta P_{pump} Q}{1714 \eta} \tag{8}$$

where η is the pump efficiency. As the drill bit progresses into the rock, the required pump horsepower increases because the distance between the drill bit and the mud pump increases and thus the total pressure drop increases. *GHGfrack* models this dynamic effect by splitting the drilling section into the desired number of segments. It calculates the energy consumption for drilling of each segment considering the changing BHP of the pump and then integrates over all these segments to calculate the total energy consumption of the mud pump for drilling the section.

2.3. Hydraulic Fracturing. Following similar principles, we can write the energy balance of hydraulic fracturing in the form of pressure drop terms:

$$\Delta P_{pump} = \Delta P_{fracturing} + \Delta P_{friction} - \Delta P_{hydrostatic} \tag{9}$$

Knowing the discharge pressure of the water injection pumps and the flow rate of the fluid (water and sand) injected, we can calculate the required BHP of the pump using eq 8. Three components drive the required discharge pressure of water pumps: the pipe friction, the fracture gradient, and the hydrostatic head of water. The fracture gradient is the amount of pressure (psi/ft) required to fracture the formation at a given depth. The fracture gradient is a property of the geologic formation. The actual discharge pressure applied can change during injection of fracturing water. *GHGfrack* considers a time average fracture gradient value as a model input. The hydrostatic head of water in the well helps to reduce the required discharge pressure of the pump.

GHGfrack models both single-stage and multistage hydraulic fracturing. In single-stage fracturing, the flow rate declines as the fluid flows from the heel of the horizontal well to the toe. The model takes this effect into account. For fracturing fluids, the Newtonian fluid model is used to calculate the pressure drop due to friction (fracturing fluids are mostly water). *GHGfrack* uses four submodules to calculate the pressure drop for the laminar and turbulent regime, and for pipe and annular flow. These equations are classic in the theory of Newtonian fluid mechanics and thus placed in the Supporting Information (section 2, eqs S8−S12). After calculation of the pressure drop across the fracturing pump, the pump BHP is calculated by eq 8.

2.4. Calculation of GHG Emissions from BHP. The results of *GHGfrack* are intended to be used by another LCA model named *OPGEE* (*Oil Production Greenhouse gas Emissions Estimator*).[3,4] To be consistent with this model, the fuel efficiency, diesel lower heating value (LHV), and emission factor are all taken from *OPGEE*.[3]

The diesel LHV is set to 128450 Btu/U.S. gal, and the emission factor is 78891 g of CO_2 eq/MMBtu LHV of diesel fuel burned, as used in the U.S. Federal GREET model.[10] *OPGEE* adopts this emission factor from *GREET* and uses (for the sake of consistency with other regulatory tools) *IPCC* AR4 global warming potential (GWP) over 100 years to estimate the equivalent CO_2 emissions (GWP CH_4 = 25; N_2O = 298).[10,11] Carbon dioxide is the dominant component with an emission factor of 77401 g of CO_2 eq/MMBtu.[3,10,12]

Equations 10−13 describe how the GHG emissions are calculated in *GHGfrack*.

$$E = \text{BHP} \times t \tag{10}$$

DOI: 10.1021/acs.est.6b01940
Environ. Sci. Technol. 2016, 50, 7913−7920

where E is the drilling energy (hp h) and t is the drilling time (h).

$$F = \frac{E\eta}{\mathrm{LHV_d}} \tag{11}$$

where F is the diesel fuel use (U.S. gal), η is the fuel efficiency of the drilling prime mover (diesel engine) (Btu LHV/BHP hr), and $\mathrm{LHV_d}$ is the diesel fuel lower heating value (Btu/gal). The fuel efficiency is approximated as a linear function of engine size:

$$\eta = 7235.4 - 0.4299S \tag{12}$$

where S is the engine size (hp). This equation is taken from *OPGEE*.[3] For a typical engine size (380−2790 hp), this equation yields a fuel efficiency of 7070 to 6035 Btu LHV diesel fuel/BHP hr. This is equivalent to an engine efficiency of 36−42%. Lastly, we model GHG emissions directly from fuel use:

$$G = F \times \mathrm{EF} \tag{13}$$

where G are GHG emissions (g of CO_2 eq) and EF is the diesel emissions factor (g of CO_2 eq/gal diesel).

3. MODEL VERIFICATION AND CALIBRATION

GHGfrack is a mechanistic model with a significant number of input variables (32 variables in total). As the exact value of many of the input variables may be unknown in any particular case, *GHGfrack* uses a few simple rules to automatically choose values of unknown key input variables from accepted ranges given in the literature based on the well geometry. To study the effectiveness of these simplifying assumptions, we compare *GHGfrack* results with published field data. Note that calibration does not mean fitting a purely statistical model to data or tuning the model by use of correction factors.

3.1. Rotation and Mud Circulation. We compare *GHGfrack* prediction against the diesel fuel consumption in drilling of oil and gas wells that Petroleum Services Association of Canada (PSAC) reported for provinces of Alberta, British Columbia, Saskatchewan, and Manitoba.[13] The reported data set consists of 23 vertical wells and 14 wells with a horizontal section. The data set provides information about the casing design, depths, and drilling time (vertical and horizontal wells are reported separately). We estimate the well geometry and effective ROPs from these data (Table S1). Other model input variables not provided by PSAC are taken from Azar and Samuel[7] (Table S2). We calibrate the model, setting the required torque for rotation of the drill string, mud flow rate, and drill collar length. Table S3 lists the simple rules used to choose these values (these values reside well within ranges of reported values from the literature).[7] In drilling the laterals, we find the best agreement between *GHGfrack* predictions and the PSAC report when only the downhole motor provides the rotational energy for the drill bit and the top driver is off. For vertical wells, the rotational energy is provided by both the top driver and the downhole motor. Note that we do not tune for each well individually but instead set calibration rules that apply across all wells. Figure 2 compares *GHGfrack* results with reported fuel consumption from PSAC. For 90% of the data for vertical drilling, *GHGfrack* predicts the diesel fuel consumption with a relative error ranging from −18.4 to 7.3%. The relative error for volume of diesel fuel consumption is defined by

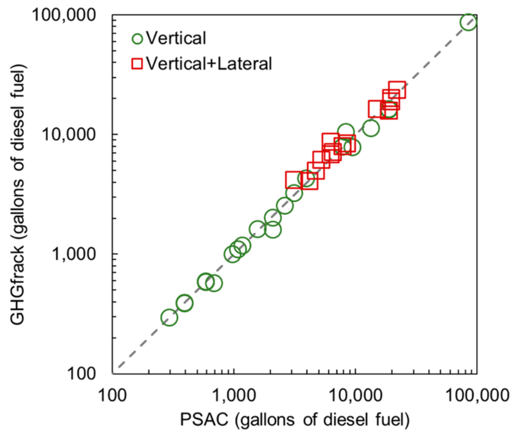

Figure 2. *GHGfrack* calibration and comparison against PSAC data.

$$\text{relative error} = \frac{\textit{GHGfrack}\ \text{prediction} - \text{PSAC reported}}{\text{PSAC reported}} \times 100 \tag{14}$$

The arithmetic average of absolute relative errors for 23 cases of vertical drilling is 7.3%. PSAC does not report separately the fuel consumption in drilling of the vertical and lateral sections. We conducted a separate calibration for drilling the laterals (curve and horizontal). The relative error in 90% of the 14 wells with horizontal drilling ranges from −9.4 to 32.7%, with an average of 10.1% (over absolute values of relative errors). Figure S1 shows the distribution of the relative errors, suggesting that *GHGfrack* is not consistently high or low in estimating fuel use.

3.2. Hydraulic Fracturing. The discharge pressure of the fracturing pump and the flow rate of the fracturing fluid are the key parameters that define the energy consumption in hydraulic fracturing. We compared the prediction of *GHGfrack* for the discharge pressure of the fracturing pump with a similar case that is simulated with *ASPEN-Hysys* using the "Pipe Segment" model for the first stage in a case of multistage fracturing.[14] The geometry of the well and the input variables for this simulation are listed in Table S4.

For the range of 500−3000 gpm of water, the relative error in estimation of the fracturing pump discharge pressure ranges from 0.1 to 2.1% (Figure S2). The agreement of the results suggests that the hydraulic module of *GHGfrack* represents Newtonian flow and friction accurately.

Next, we compare the results of the fracturing module with field data taken from a report prepared by the Eastern Research Group (ERG) for the Texas Commission on Environmental Quality (TCEQ).[15] We use data collected from four companies on energy consumption for hydraulic fracturing of gas and oil zones of the Eagle Ford shale play. The total horsepower, number of the fracturing stages, and duration of fracturing per stage are reported. We calculate the diesel fuel used from the reported data. We assume each fracturing stage is 300 ft and on this basis estimate the length of the horizontal section (Table S5). To account for missing data, we assume an average geometry of the wells of the Engle Ford, and the rest of the model inputs are from the literature (Table S6).[7,16,17] We leave one degree of freedom, which is the flow rate of the fracturing fluid in GPM.

Figure 3 compares the diesel fuel consumption for running fracturing pumps estimated by *GHGfrack* against the ERG

DOI: 10.1021/acs.est.6b01940
Environ. Sci. Technol. 2016, 50, 7913−7920

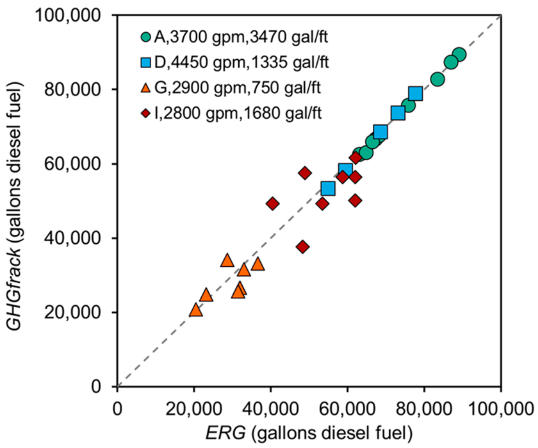

Figure 3. Comparison of the *GHGfrack* estimates for diesel fuel consumption in a hydraulic fracturing operation with an ERG-collected report. The flow rates of fracturing fluid injected both in gpm and in per foot of the horizontal well are given for companies A, D, G, and I.

report for four companies with pseudonyms of A, D, G, and I.[15] The overall relative error for 90% of data from all the four companies ranges from −18.7 to 17.9%. The arithmetic mean of absolute relative errors is 7.1%. While the data points from companies G and I are scattered more naturally around the diagonal line on the parity chart, the data from companies A and D demonstrate a nearly perfect relationship. This might lead one to question whether the data provided by companies A and D are in fact field data or are generated using an empirical equation. The arithmetic mean of the absolute value of relative errors for companies A, D, G, and I, when calculated separately for their individual set of data, are 1.0, 3.7, 11.9, and 12.8%, respectively.

The calculated average injection rates in terms of gallons per foot of horizontal section for each company are also given in Figure 3. Scanlon et al. provide a map of Eagle Ford play that indicates the use of hydraulic fracturing water in terms of gallons per foot.[18] Water consumption is reported in the range of 500−2500 gal/ft. According to this map, water consumption of <500 and >2500 gal/ft is still possible and marked on the map. The average water consumption as a consequence of adjustment of the flow rate for companies D, G, and I is between 750 and 1680 gal/ft, which is consistent with Scanlon's map. The water consumption by company A on average is estimated to be 3470 gal/ft, which is above 2500 gal/ft. According to ERG, this company is operating in Dimmit, Webb, and Maverick counties.[15] Scanlon's map shows that there is an area nearly shared by these counties that is marked densely for water consumption above 2500 gal/ft, at odds with the rest of the Eagle Ford play.[18] We conclude that the mechanistic fracturing module that we developed for *GHGfrack* can be tuned with only one free variable (fracturing fluid flow rate), and therefore, the *GHGfrack* results are consistent with independent published data.

4. RESULTS AND DISCUSSION

4.1. Case Studies of Bakken and Eagle Ford. To demonstrate the use of *GHGfrack*, we run two illustrative case studies with large numbers of wells. Data are gathered for 6927 wells in the Eagle Ford play and for 4431 wells in the Bakken play. The Eagle Ford play consists of different zones of gas,

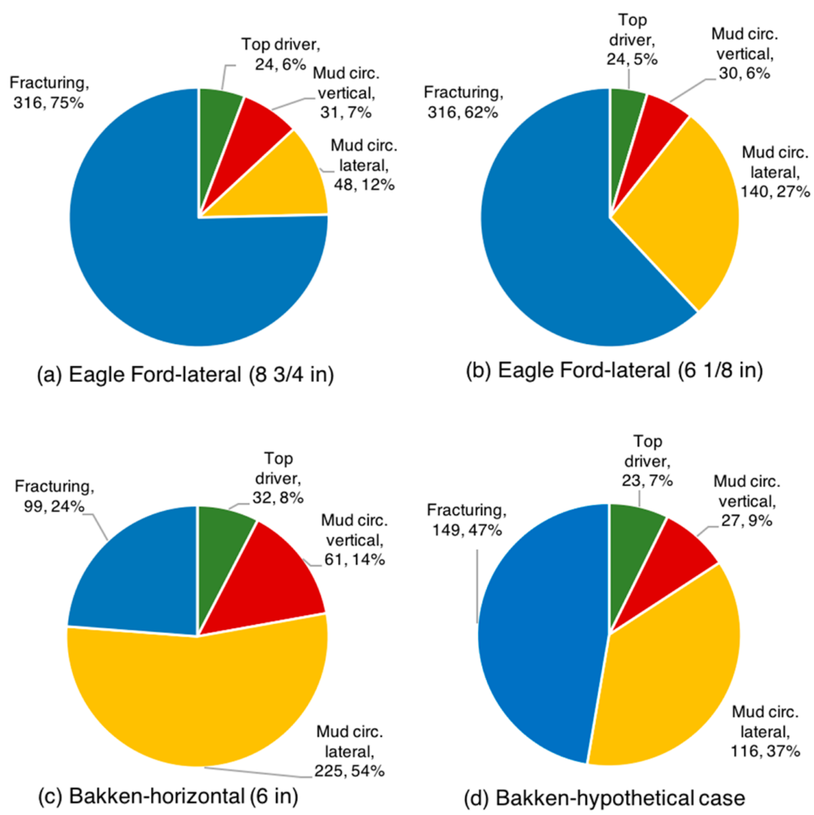

Figure 4. Case studies of Eagle Ford and Bakken. The breakdown of emissions from combustion of diesel fuel to supply energy for drilling and hydraulic fracturing is given in metric tonnes of CO_2 eq/well together with the percentage of the total emissions from the indicated activities.

DOI: 10.1021/acs.est.6b01940
Environ. Sci. Technol. 2016, 50, 7913−7920

condensate, and oil wells.[16,18] The volume of the fracturing fluid injected and the length of the vertical and the laterals are given for each well, with data derived from two studies about emissions from production of petroleum from these two fields sponsored by Argonne National Laboratory (Tables S7 and S8).[16,19] The geometry of wells and hole sizes are taken from Guo et al. and Jellison et al. for Eagle Ford and Bakken, respectively.[17,20] The rest of the model inputs are the same as those we used in the PSAC model calibration described above (Table S2). We assume the same average injection time is spent in fracturing of each stage (300 ft) in both Eagle Ford and Bakken. The injection time, 2.6 h per fracturing stage, is the average over the collected data from the four companies reported by ERG.[15] ROPs during vertical and horizontal drilling are different and are the averages taken from ERG.[15] The same injection time per stage and ROPs are used for the case of Bakken (Table S9).

These results should be considered only illustrative, not exact. For example, there is no reason to assume that the model input variables in drilling or fracturing for an entire oil play would be the same. Also, the calibration data from Canadian provinces may differ from those of plays in the northern and southern United States. Therefore, the goal of these two case studies is not to compute the precise emissions from these two oil fields but instead to investigate model behavior in response to significant differences between the Eagle Ford and Bakken drilling and fracturing operating conditions and the formation characteristics.

We run *GHGfrack* for two well geometries in Eagle Ford with lateral sizes of 8 $^3/_4$ and 6 $^1/_8$ in. In the case of Bakken, the size of the horizontal section is 6 in. Figure 4 presents the average of the resulting distributions. The given size of the lateral (drilling hole diameter) in Figure 4 is related to drilling operation. In fracturing operations in the case of Eagle Ford, the fluid is injected through a casing with an internal diameter (ID) of 5 in. (the entire path from the well head to the fracturing zone).[17] In the case of Bakken, the fracturing fluid is injected through a vertical casing with an ID of 6 $^1/_8$ in. and through a lateral casing with an average ID of 4 in.[20] The model outputs are given in detail in Table S10. Figure 4a shows the breakdown of the combustion GHG emissions for the most common well design in Eagle Ford according to Guo et al. (65% of Eagle Ford wells).[17] The total GHG emissions for the first Eagle Ford case with an 8 $^3/_4$ in. lateral is 419 metric tonne of CO_2 eq/well. As the lateral hole size decreased from 8 $^3/_4$ to 6 $^1/_8$ in. in the second case study of Eagle Ford, the total GHG emissions increase to 510 tonne of CO_2 eq/well (Figure 4b). A 21% increase in energy consumption for mud circulation in the lateral section is observed, which is equivalent to emission of an extra 92 tonne of CO_2 eq/well. This increase is due to an larger pressure drop in mud flow in narrow diameter laterals.

Figure 4c shows that the energy consumption in Bakken for mud circulation is significantly higher and in fracturing significantly lower than the energy consumption in both Eagle Ford case studies. The average length of the horizontal section in Bakken is 9190 ft and in Eagle Ford is 4792 ft. The longer size of the horizontal section requires longer times for drilling and mud circulation and explains the significantly higher mud pump energy consumption. The longer size of the lateral can increase the total pressure drop due to pipe friction; however, in comparison with other lateral sizes, diameter is a key variable. The much greater energy requirement for fracturing in Eagle Ford is due to the fact that average volume of the fracturing fluid injected is much greater than the volume injected in the case of Bakken, 2.7 million U.S. gal/well in Bakken and 5.0 million U.S. gal/well in Eagle Ford. We examine a hypothetical case in which we run *GHGfrack* for the Bakken case with Eagle Ford average vertical and lateral well depths. The results are depicted in Figure 4d. Comparing those results with Figure 4b in which the diameter of the lateral is closer to the case of Bakken, we see the energy consumption in drilling in both cases become more similar. The energy consumed in fracturing increases but remains significantly lower than that of Eagle Ford. This illustrates the sensitivity of *GHGfrack* results both to the volume of the injected fracturing fluid and to the length of the lateral.

The estimated ultimate recoveries (EURs) of oil for 4431 Bakken wells that we studied are 169−767 Mbbl (95% confidence interval) and for 6927 Eagle Ford wells 174−454 Mbbl.[16,19] The mean values of EUR for these wells are 252 and 250 Mbbl for Bakken and Eagle Ford, respectively. These data are limited to the wells that we studied and do not represent the entire Bakken and Eagle Ford plays. The GHG emissions from combustion of diesel fuel for the first three cases that are shown in Figure 4 are 1.0−5.3 kg of CO_2 eq/bbl for the case of Eagle Ford with an 8 $^3/_4$ in. lateral with a mean value of 1.9 kg of CO_2 eq/bbl, 1.4−5.9 kg of CO_2 eq/bbl for the case of Eagle Ford with a 6 $^1/_8$ in. lateral with a mean value of 2.3 kg of CO_2 eq/bbl, and 1.4−6.9 kg of CO_2 eq/bbl for the case of Bakken with a mean value of 2.3 kg of CO_2 eq/bbl. The total GHG emissions from combustion of diesel fuel for these three cases are 419, 510, and 417 tonne of CO_2 eq/well, respectively. An area of future study might be the relationship between the ultimate recovery of hydrocarbons and energy consumption during drilling and fracturing. That is, does energy expenditure on additional well complexity, length, or fracturing cause commensurate increases in productivity? Future work could couple a model like *GHGfrack* to a reservoir simulation tool providing that rich sets of data of operation, well geometry, and ultimate gas and oil recovery for each well are available.

Considering the EUR for each well, the results can be expressed in terms of ultimate oil recovery volume, or the equivalent heating value. We have used *GHGfrack* for net energy analysis of Bakken crude oil production in a previously published article.[21]

4.2. Sensitivity Analysis. *GHGfrack* has 32 model input variables, some of which may remain uncertain without detailed operator data. To explore the impacts of uncertainty in knowing the exact value of the input variables, we conduct a single-variable sensitivity analysis using the average input values from the Eagle Ford case study as the baseline. The input variables are listed in Tables S2, S3, S7, and S9. The input variables are changed ±10%, one at a time, and resulting changes in energy consumption are recorded. Figure 5 shows the results of the sensitivity analysis. Only input variables that caused a more than ±5% change in energy consumption are depicted in this figure. Given that only 15 variables are shown in Figure 5, we can surmise that half of the input variables are not significant drivers of emissions (e.g., drilling mud density and viscosity).

Three input variables cause a change of >15% in total energy consumed in drilling (top driver and mud pump): lateral hole ID, drill pipe ID, and mud flow rate in the horizontal section (Figure 5a). Two input variables cause a more than ±15% change in fracturing pump energy consumption: lateral casing diameter and fracturing fluid volume (Figure 5b).

DOI: 10.1021/acs.est.6b01940
Environ. Sci. Technol. 2016, 50, 7913−7920

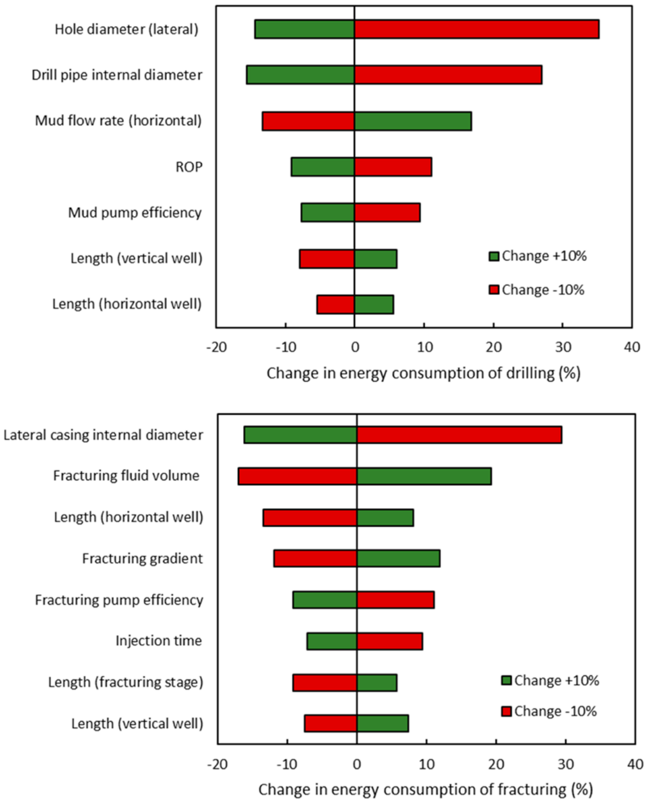

Figure 5. Sensitivity analysis. ROP refers to the rate of penetration of the drill bit into rock.

Figure 5 also shows the nonlinearity of the system: a change of 10% in an input variable can cause a less or more than 10% change in the output. In a nonlinear system, the sensitivity to the change of a certain input variable depends on the initial state of the system; in other words, the value of the input variables before the perturbation affects the degree of perturbation experienced. In this case, a single-variable sensitivity analysis cannot be considered as the ultimate tool to determine the overall certainty of the model results, and a multivariable sensitivity analysis accounting for physical correlation between input variables should eventually be performed. For an example of multivariable analysis of uncertainty resulting from the lack of knowledge of model inputs of a nonlinear LCA model, see ref 22.

The GHG emissions estimates in this article are limited to emissions from combustion of diesel fuel for supplying energy only for rotation of the drill string, drilling mud circulation, and fracturing pumps. In a future work, we will investigate the methane and other GHG emissions from the flow back process and fugitive emissions from underbalance drilling.

■ ASSOCIATED CONTENT

Supporting Information

The Supporting Information is available free of charge on the ACS Publications website at DOI: 10.1021/acs.est.6b01940.

Additional equations, tables, figures, and references (PDF)

GHGfrack is an open-source model (XLS)

■ AUTHOR INFORMATION

Corresponding Author

*E-mail: vafi@stanford.edu. Phone: 650-518-9771.

Notes

The authors declare no competing financial interest.

■ ACKNOWLEDGMENTS

This research is sponsored by the California Air Resources Board (CARB), a division of the California Environmental Protection Agency (CalEPA), under sponsored research project 13-408. We greatly appreciate the contributions of Jim Duffy (CARB) to this project.

■ REFERENCES

(1) Annual Energy Outlook 2015 with projections to 2040, DOE/EIA-0383(2015), April 2015.

(2) Osborn, S. G.; Vengosh, A.; Warner, N. R.; Jackson, R. B. Methane contamination of drinking water accompanying gas-well drilling and hydraulic fracturing. *Proc. Natl. Acad. Sci. U. S. A.* **2011**, *108* (20), 8172−8176.

(3) El-Houjeiri, H.; Vafi, K.; Duffy, J.; McNally, S.; Brandt, A. *Oil Production Greenhouse Gas Emissions Estimator OPGEE*, version 1.1, draft D, 2014.

(4) El-Houjeiri, H.; Brandt, A.; Duffy, J. Open-source LCA tool for estimating greenhouse gas emissions from crude oil production using field characteristics. *Environ. Sci. Technol.* **2013**, *47*, 5998−6006.

(5) Howarth, R. W.; Ingraffea, A.; Engelder, T. Natural gas: Should fracking stop? *Nature* **2011**, *477* (7364), 271−275.

(6) Caulton, D. R.; Shepson, P. B.; Santoro, R. L.; Sparks, J. P.; Howarth, R. W.; Ingraffea, A. R.; Cambaliza, M. O.; Sweeney, C.; Karion, A.; Davis, K. J.; Stirm, B. H.; Montzka, S. A.; Miller, B. R. Toward a better understanding and quantification of methane emissions from shale gas development. *Proc. Natl. Acad. Sci. U. S. A.* **2014**, *111* (17), 6237−6242.

(7) Azar, J. J.; Samuel, R. *Drilling engineering*; PennWell: Tulsa, OK, 2007.

(8) Halliburton downhole drilling motors (http://www.halliburton.com/en-US/ps/sperry/drilling/directional-drilling/downhole-drilling-motors/default.page?node-id=hfvq7ixp) (accessed April 2016).

(9) Mitchel, R. F., Ed. *Petroleum engineering handbook*; Society of Petroleum Engineers: Richardson, TX, 2006; Vol. *II*.

(10) GREET model (https://greet.es.anl.gov/) (accessed April 2016).

(11) IPCC 2007 (https://www.ipcc.ch/publications_and_data/ar4/wg1/en/ch2s2-10-2.html) (accessed April 2016).

(12) Development of Baseline Data and Analysis of Life Cycle Greenhouse Gas Emissions of Petroleum-Based Fuels. DOE/NETL-2009/1346; 2008.

(13) 2013 Well Cost Study; Petroleum Services Association of Canada (PSAC): Calgary, AB, 2013.

(14) *ASPEN-Hysys*, version 8.8 (http://www.aspentech.com/products/aspen-hysys/) (accessed April 2016).

(15) Pring, M.; Baker, R.; Oommen, R.; Preusse, D. 2014 statewide drilling rig emissions inventory with updated trends inventories; Eastern Research Group (ERG): Lexington, MA, 2015.

(16) Ghandi, A.; Yeh, S.; Brandt, A. R.; Vafi, K.; Cai, H.; Wang, M. Q.; Scanlon, B. R.; Reedy, R. C. Energy intensity and greenhouse gas emissions from crude oil production in the Eagle Ford region: Input data and analysis methods. Argonne National Laboratory: Argonne, IL, 2015 (https://greet.es.anl.gov/publication-eagle-ford-oil) (accessed April 2016).

(17) Guo, Q.; Ji, L.; Rajabov, V.; Friedheim, J. E.; Portella, C.; Wu, R. Shale gas drilling experience and lessons learned from Eagle Ford. SPE 155542, in SPE Americas Unconventional Resources Conference; Society of Petroleum Engineers: Richardson, TX, 2012.

DOI: 10.1021/acs.est.6b01940
Environ. Sci. Technol. 2016, 50, 7913−7920

(18) Scanlon, B. R.; Reedy, R. C.; Nicot, J. P. Comparison of water use for hydraulic fracturing for unconventional oil and gas versus conventional oil. *Environ. Sci. Technol.* **2014**, *48* (20), 12386−12393.
(19) Brandt, A. R.; Yeskoo, T.; McNally, S.; Vafi, K.; Cai, H.; Wang, M. Q. Energy intensity and greenhouse gas emissions from crude oil production in the Bakken formation: Input data and analysis methods. Argonne National Laboratory: Argonne, IL, 2015 (https://greet.es.anl.gov/publication-bakken-oil) (accessed April 2016).
(20) Jellison, M.; Brock, J.; Muradov, A.; Morgan, D.; Rowell, J. Shale play drilling challenges: Case histories and lessons learned. SPE/IADC 163447, in SPE/IADC Drilling Conference; Society of Petroleum Engineers: Richardson, TX, 2013.
(21) Brandt, A. R.; Yeskoo, T.; Vafi, K. Net energy analysis of Bakken crude oil production using a well-level engineering-based model. *Energy* **2015**, *93*, 2191−2198.
(22) Vafi, K.; Brandt, A. R. Uncertainty of oil field GHG emissions resulting from information gaps: A Monte Carlo approach. *Environ. Sci. Technol.* **2014**, *48* (17), 10511−10518.

DOI: 10.1021/acs.est.6b01940
Environ. Sci. Technol. 2016, 50, 7913−7920